Ionic Liquid-assisted Isolation of Lignin From Lignocellulose and Its Esterification with Fatty Acids

Eun-Ah Lee,[a] Jeong-Ki Kim,[a] Rajkumar Bandi,[b] Ramakrishna Dadigala,[b] Song-Yi Han,[b] Gu-Joong Kwon,[b,c] Jaegyoung Gwon,[d] Won-Jae Youe,[d] Ji-Soo Park,[d] Chan-Woo Park,[b] Nam-Hun Kim,[a,b] and Seung-Hwan Lee [a,b,c,*]

Ionic liquids (ILs) have been widely used for lignocellulose fractionation and lignin isolation. However, the effect of IL treatment on lignin structure has been less explored. This study aimed to explore the chemical structure of lignin isolated by widely used imidazolium based ILs and compare it with the well-known milled wood lignin structure (MWL). Four types of ILs were used, and the effects of the treatment conditions on the isolated lignin (ILL) characteristics were evaluated. As the treatment temperature was increased from 60 to 140 °C, the ILL yield increased, whereas the molecular weight and hydroxyl group content decreased. Among the ILs, [EMIM]Ac produced the highest lignin yield (5.28%), and the ILL obtained had the lowest hydroxyl content (1.27 mM/g) and a molecular weight (M_w) of 29,500 g/mol. Esterification of the ILL isolated with [EMIM]Ac was performed using three fatty acid chlorides, octanoyl chloride (C_8), lauroyl chloride (C_{12}), and palmitoyl chloride (C_{16}), to extend its applicability. The effects of esterification on the characteristics of ILL were evaluated, and successful esterification was confirmed using Fourier transform infrared and nuclear magnetic resonance spectroscopies.

DOI: 10.15376/biores.17.4.5861-5877

Keywords: Ionic liquids; Lignin isolation; Temperature effect; Lignin esterification

*Contact information: a: Department of Forest Biomaterials Engineering, College of Forest and Environmental Sciences, Kangwon National University, Chuncheon, 24341, Republic of Korea; b: Institute of Forest Science, Kangwon National University, Chuncheon, 24341, Republic of Korea; c: Kangwon Institute of Inclusion Technology, Kangwon National University, Chuncheon, 24341, Republic of Korea; d: Division of Forest Industrial Materials, Department of Forest Products and Industry, National Institute of Forest Science, Seoul, 02455, Republic of Korea; *Corresponding author: lshyhk@kangwon.ac.kr*

INTRODUCTION

Lignocellulose is the most abundant renewable bioresource on earth; it is mainly composed of cellulose (40% to 60%), hemicellulose (25% to 35%), and lignin (15% to 30%) (Isikgor and Becer 2015). Lignocellulose has attracted considerable attention as a potential biomaterial to replace petrochemical-based materials such as synthetic plastics (Su *et al.* 2018; Tanase-Opedal *et al.* 2019; Yang *et al.* 2019). The advantages of lignocellulose are not only that it is a non-food feedstock that does not compete with food resources, but it is also considered a carbon-neutral material, as carbon dioxide is absorbed during its growth.

Lignin is the most abundant aromatic natural polymer on earth. Typically, the lignin content of softwoods is approximately 25% to 35%, and that of hardwoods is approximately 20% to 30%. Lignin surrounds cellulose and hemicellulose, maintains the wood cell wall, and acts as a barrier to prevent the intrusion of pathogens (Vanholme *et al.*

2010). Lignin is an amorphous polyphenolic polymer composed of randomly polymerized phenylpropanoid units, namely coniferyl alcohol, sinapyl alcohol, and p-coumaryl alcohol (Sannigrahi *et al.* 2010). Lignins with high molecular weights are difficult to isolate because of their highly complex structure, which is covalently linked to hemicellulose to form a lignin–carbohydrate complex (You *et al.* 2015; Tarasov *et al.* 2018).

Lignin is commonly obtained by the kraft pulping process, which uses severe treatment conditions. Lignin can be collected by acidifying black liquor in the kraft pulping process. This method has many disadvantages, such as the requirement for hazardous reagents and intensive energy consumption (An *et al.* 2015). The most fatal problem limiting the effective utilization of lignin is its irreversible condensation during the extraction and separation processes (Zakzeski *et al.* 2010). Consequently, although a large amount of lignin is obtained through this pulping process, most of this is burned to provide energy for the mill operation, and only small amounts (approximately 1% to 2%) are used to produce valuable products. Therefore, it is necessary to develop a new isolation method for lignin, which can be used as a highly functional material.

Ionic liquids (ILs) are effective non-derivative pretreatment solvents for lignocellulose because of their powerful ability to dissolve cellulose, lignin, and even whole lignocellulose (Brandt *et al.* 2013). Additionally, ILs can isolate lignin from lignocellulose without high energy consumption and do not lead to the condensation of lignin structures (Sathitsuksanoh *et al.* 2014). The ILs are salts that exist in the liquid state at or below 100 °C and are formed by ionic bonds between cations and anions. Recently, ILs have attracted attention because of their advantages of eco-friendliness, excellent biopolymer solubility, thermal stability, non-volatility, and electrical conductivity (Yuan *et al.* 2018).

Many researchers have reported on the fractionation of lignocellulose using a series of ILs (Dong *et al.* 2015; Xu *et al.* 2015; Zhang *et al.* 2015; Audu *et al.* 2017). Most of these studies were focused on increasing delignification and improving enzymatic digestibility of cellulose rich residue. However, studies on impact of IL extraction on lignin structure are rare (Audu *et al.* 2017). In view of the great research interest in using ILs for lignocellulose pretreatment, exploration of IL effect on lignin chemical structure that can provide structural details and mechanistic insights is of great significance.

Lignin can be used in many fields, including pharmaceuticals, natural antioxidants, additives, and dispersants (Cateto *et al.* 2011; Delmas *et al.* 2013; Yu and Kim 2020). However, raw lignin, *i.e.*, chemically unmodified lignin, has poor solubility in organic solvents and poor compatibility with other polymers. The esterification of lignin can be used to improve these properties.

This study aimed to explore the chemical structure of lignin isolated by widely used imidazolium based ILs and compare it with the milled wood lignin structure (MWL), which is known as the most similar lignin to native lignin. Esterification with long chain fatty acids is known to improve the hydrophobicity and compatibility with other polymers. Hence, to further extend the applicability of as isolated lignin (ILL), esterification with three fatty acid chlorides of different molecular chain lengths (C8, C12, and C16) was also demonstrated.

EXPERIMENTAL

Materials

Quercus mongolica Fisch. ex Ledeb. was supplied as lignocellulose by the National Institute of Forest Science (Seoul, Republic of Korea). Wood powder with a 40- to 80-mesh size (180 to 425 μm) was prepared and extracted using ethanol/benzene (1:2, v/v) at 90 °C for 8 h to remove extractives prior to treatment with IL. Four types of ILs, namely 1-ethyl-3-methylimidazolium acetate ([EMIM]Ac) (≥ 98%), 1-allyl-3-methylimidazolium chloride ([AMIM]Cl) (≥ 98%), 1-butyl-3-methylimidazolium chloride ([BMIM]Cl) (≥ 99%), and 1-hexyl-3-methylimidazolium chloride ([HMIM]Cl) (≥ 98%), were purchased from IoLiTec (Heilbronn, Germany). Chloroform-d ($CDCl_3$, ≥ 99.96 atom % D) was obtained from Sigma-Aldrich (St. Louis, MO, USA). Three types of fatty acid chlorides—octanoyl chloride (OC) (> 99%), lauroyl chloride (LC) (> 98%), and palmitoyl chloride (PC) (> 97%)— were purchased from TCI Co., Ltd. (Tokyo, Japan). Ethyl alcohol (> 94.5%), benzene (> 99.5%), acetone (> 99.5%), 1-n hydrochloric acid standard solution, pyridine (> 99.5%), acetic anhydride (> 97%), 1,4-dioxane (> 99.5%), acetic acid (> 99.5%), tetrahydrofuran (THF, > 99.5%), *N*,*N*-dimethylformamide (DMF, > 99.5%), dimethyl sulfoxide (DMSO), and anhydrous lithium bromide (LiBr) were obtained from Daejung Chemical & Metals Co., Ltd. (Siheung, Republic of Korea).

Isolation of MWL

The MWL was prepared for comparison with the characteristics of the ILLs. Lignocellulose (10 g) was ball-milled at 450 rpm for 3 h with a pause every 10 min using ZrO_2 bowls and ZrO_2 balls in a planetary ball mill (Fritsch, Idar-Oberstein, Germany). The milled wood powder was added to 96% aqueous 1,4-dioxane (200 mL) and stirred for 24 h. The suspension was then vacuum filtered using 1,4-dioxane, and the filtrate was evaporated under vacuum to remove the 1,4-dioxane. The concentrated filtrate was added dropwise to water and regenerated by stirring to obtain crude MWL. The crude MWL was dissolved in 90% acetic acid (30 mL/g crude MWL) with stirring. The solution was dropped into water, and the precipitated residue (MWL) was collected by vacuum filtration with water. A schematic of the MWL isolation process is presented in Fig. 1.

Ionic Liquid-assisted Isolation of Lignin

Lignocellulose was added to the ILs at a solid loading of 15 wt% and reacted at 60, 100, 120, and 140 ℃ for 2 h. An acetone/water (1/1, v/v) solution was slowly added to the treatment slurries, and the mixture was stirred for 1 h at room temperature. Then, the IL insoluble fraction (polysaccharide-rich) was filtered out, washed with an excess of acetone/water (1/1, v/v), and stored at 40 ℃ under vacuum after freeze-drying. The solubility in acetone/water was calculated using the weights of the raw material and insoluble fraction in the process. The filtrate (lignin-rich fraction) was evaporated at 50 ℃ under vacuum to remove the acetone, adjusted to pH 2 using 1 M HCl, and left to stand for 48 h to precipitate the lignin. The precipitated lignin was washed, filtered with distilled water, and dried at 40 ℃ under vacuum after freeze-drying. The lignin isolated using ILs was named ILL. The yield of ILL was calculated using Eq. 1. A flowchart of the ILL isolation process is shown in Fig. 1.

$$\text{Yield (\%)} = \text{Weight of ILL (g)} / \text{Weight of raw material} \times 100 \quad (1)$$

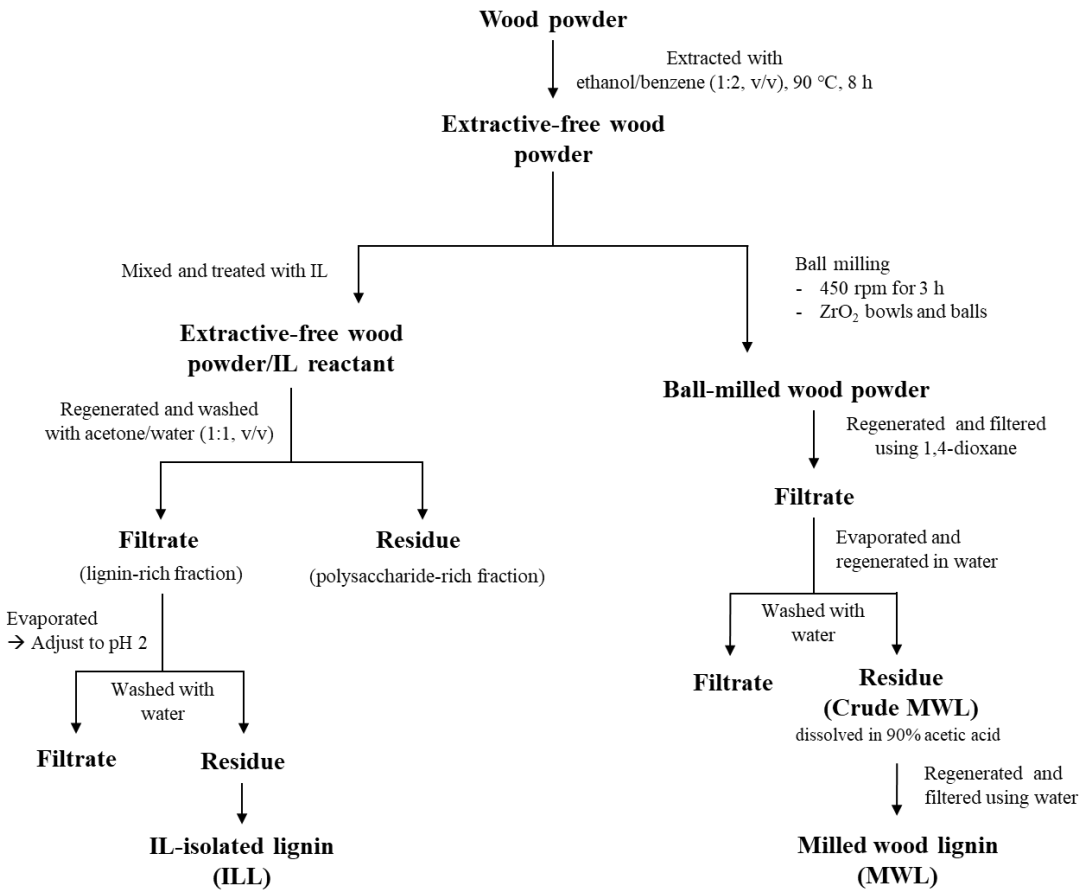

Fig. 1. Flowchart of the ILL and MWL isolation processes

Esterification of ILL

The esterified ILL was prepared as described previously by Koivu *et al*. (2016). The ILL isolated using [EMIM]Ac at 140 ℃ for 2 h was used as the raw material for esterification. The ILL (0.5 g) was dissolved for 30 min in a mixture (18.8 mmol/g ILL) of THF, DMF, and pyridine at 60 ℃ under nitrogen gas. Fatty acid chlorides with different chain lengths (OC (C_8), LC (C_{12}), and PC (C_{16})) were injected with a syringe at concentrations of 2.0 equivalents relative to the total aliphatic and phenolic hydroxyl groups. The reaction was allowed to proceed at 60 °C for 48 h under nitrogen gas with stirring. The reactant was dropped into water for regeneration, followed by washing with water and ethanol. The esterified ILL was freeze-dried. The ILLs esterified using OC, LC, and PC are denoted OC-ILL, LC-ILL, and PC-ILL, respectively.

Chemical Composition

The lignin content of lignocellulose was measured using the Klason method. A total of 1 mL of 72% H_2SO_4 was added to 200 mg of lignocellulose and stirred for 2 h. The mixture was diluted with 112 mL of distilled water to decrease the concentration to 3%, followed by secondary hydrolysis in an autoclave at 120 ℃ for 1 h. After the reaction, the acid-insoluble fraction (Klason lignin) was collected by vacuum filtration using a glass filter and washed with an excess of distilled water until a neutral pH was achieved to remove residual acid.

The monosaccharide contents, including arabinose, galactose, glucose, xylose, and mannose, were determined using high-performance ion chromatography (Bio-LC, ICS-3000; Dionex, Sunnyvale, CA, USA) connected to an electrochemical detector using pulsed amperometry (gold electrode). The sample was then separated on a CarboPac PA-1 chromatography column (Dionex, Sunnyvale, CA, USA). The system was operated in isocratic mode at a flow rate of 1.0 mL/min with a mixture of 250 mM sodium hydroxide (20%) and deionized water (80%). The contents of glucose (corresponding to cellulose) and xylose, galactose, arabinose, and mannose (corresponding to hemicellulose) were calculated using the Chromeleon software program (version 6.8; Dionex, Sunnyvale, CA, USA). The cellulose and hemicellulose contents were calculated based on these monosaccharide contents.

Characterization

Acetylation of the lignin samples was conducted by mixing 100 mg of sample, 4 mL of pyridine, and 4 mL of acetic anhydride, followed by stirring for 12 h. The acetylated lignin was then added dropwise to 400 mL of water, stirred for 30 min, and washed with water. Freeze-dried ILLs were subjected to gel permeation chromatography (GPC), gas chromatography with flame ionization detection (GC/FID), and ^{1}H nuclear magnetic resonance (^{1}H NMR) analyses.

For the GPC analysis, 1 mg of acetylated lignin sample was dissolved in 1 mL of DMSO containing 0.1% LiBr and filtered using a syringe filter. The molecular weight was analyzed by GPC (Prominenece-I GPC system; Shimadzu, Kyoto, Japan) equipped with a PLgel 5 μm mixed-C, -D, and PLgel 3 μm mixed-E column using a 280 nm UV detector. Polystyrenes with a molecular weight range of 1480 to 1,233,000 g/mol were used to create a calibration curve.

The methoxyl group content of the lignin was analyzed using GC/FID. Thirty milligrams of acetylated ILLs were added to hydrioidic acid and reacted at 130 ℃ for 30 min with stirring. Then, 200 μL of internal standard (300 mg/mL ethyl iodide in pentane) was added to the cooled reactant, followed by 3 mL of pentane. The entire solution was stirred sufficiently, and part of the phase-separated solution was collected. The GC/FID was performed on a FID-7890B (Agilent Technologies, Santa Clara, CA, USA) instrument equipped with a DB-624 column (30 × 0.25 mm^2). The injector temperature was 200 ℃, and the detector temperature was 230 ℃. Using the internal standard, a calibration curve was created from the related area of CH_3I/IS and the mass of CH_3I/IS was used to determine the influence factor coefficient.

Fourier transform infrared (FT-IR) spectra were recorded on a Frontier (PerkinElmer, Beaconsfield, Buckinghamshire, UK) instrument in the range of 4000 to 400 cm^{-1} using 128 scans. The structure of lignin was investigated using ^{1}H NMR (Bruker Avance II 600 MHz, Bruker, Ettlingen, Germany). A total of 20 mg of ILL was dissolved in 1.5 mL $CDCl_3$ and filtered using a syringe filter. The hydroxyl groups were calculated by comparing the methoxyl group and acetylated OH group. Thermogravimetric analysis was performed using a thermal analysis system (SDT Q600, TA instruments, New Castle, DE, USA). The esterified ILL was tested under a nitrogen atmosphere at a heating rate of 10 ℃/min from room temperature to 700 ℃.

RESULTS AND DISCUSSION

Chemical Composition

Table 1 presents the chemical composition of the raw material. The lignin content was calculated using the Klason method, and the cellulose and hemicellulose contents were calculated based on the monosaccharide contents. The raw material consisted of 50.6% cellulose, 28.0% hemicellulose, and 21.4% lignin.

Table 1. Chemical Composition of Raw Material

Cellulose (%)	Hemi-cellulose (%)	Klason Lignin (%)	Monosaccharide Content (%)					
			Arabinose	Galactose	Glucose	Xylose	Mannose	Total
50.6	28.0	21.4	0.9	2.3	64.4	32.1	0.2	100.0

Yields of ILLs

The acetone/water solubility and yields of the ILLs obtained under different treatment conditions are summarized in Table 2; both quantities were calculated based on the weight of the raw material. When treated with [EMIM]Ac, the acetone/water solubility increased as the treatment temperature increased, and the highest acetone/water solubility (9.86%) was obtained at 140 °C. When treated with [AMIM]Cl, [BMIM]Cl, and [HMIM]Cl, the acetone/water solubilities were 3.03%, 5.35%, and 7.74%, respectively. Under the same conditions, the solubility was in the order of [EMIM]Ac > [HMIM]Cl > [BMIM]Cl > [AMIM]Cl, indicating that [EMIM]Ac had the greatest ability to dissolve lignocellulose. The effects of different treatment temperatures and types of ILs on the ILL yields were also investigated. The yield of ILL increased as the treatment temperature increased, and the highest yield of 5.28% was obtained at 140 °C. Under the same IL treatment conditions, the highest yield of ILL (5.28%) was obtained using [EMIM]Ac. The yields of the ILLs isolated with [AMIM]Cl, [BMIM]Cl, and [HMIM]Cl were 1.66%, 1.55%, and 1.52%, respectively, showing no remarkable differences.

Table 2. Acetone/Water Solubility and Yields of ILLs

IL	Reaction Temperature (°C)	Acetone/Water Soluble Fraction (%)	Yield of ILL (%)
[EMIM]Ac	60	6.51	0.64
	100	7.61	1.25
	120	9.68	1.95
	140	9.86	5.28
[AMIM]Cl	140	3.03	1.66
[BMIM]Cl	140	5.35	1.55
[HMIM]Cl	140	7.74	1.52

Note: Reaction time, 2 h; Solid loading, 15 wt%

Structural Analysis of MWL and ILLs

Figure 2 shows the FT-IR spectra for the MWL and ILLs. Peaks were detected at 3400, 2926, 1713, 1595, 1506, 1453, 1421, 1326, 1216, 1119, and 1029 cm^{-1}. The ILLs exhibited a broad band in the range of 3000 to 3600 cm^{-1}, which can be assigned to O-H

stretching vibrations. This is attributed to the presence of alcohol and phenolic hydroxyl groups. The peak at 2926 cm^{-1} is related to C-H stretching in the methoxyl groups. The peak at 1713 cm^{-1} is attributed to the unconjugated carbonyl group (C=O stretching). The absorption bands located at approximately 1600 and 1500 cm^{-1} are related to the aromatic rings of lignin. The peaks at 1595, 1506, and 1421 cm^{-1} are attributed to the aromatic skeletal vibration, which are typical peaks of lignin, and the peak at 1453 cm^{-1} is related to C-H deformation. These peaks indicate that the basic structure of the lignin was not damaged during the isolation process using ILs. The peak at 1326 cm^{-1} is associated with C-O stretching of the syringyl unit, and the peak at 1029 cm^{-1} is assigned to C-O deformation (Awal and Sain 2011). The ILLs exhibit the typical FT-IR spectrum of the MWL molecular structure, which is known as the most similar lignin to native lignin, indicating that there was no damage or minimal damage to the lignin structure during extraction using ILs.

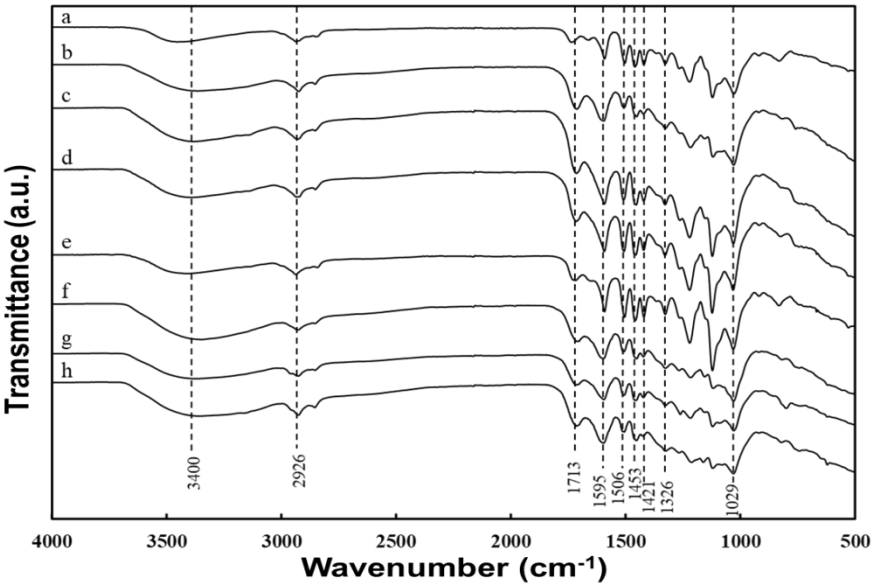

Fig. 2. FT-IR spectra of MWL and ILLs: **(a)** MWL; **(b)** [EMIM]Ac, 60 °C; **(c)** [EMIM]Ac, 100 °C; **(d)** [EMIM]Ac, 120 °C; **(e)** [EMIM]Ac, 140 °C; **(f)** ([AMIM]Cl, 140 °C; **(g)** [BMIM]Cl, 140 °C; **(h)** [HMIM]Cl, 140 °C (Note: reaction time, 2 h; solid loading, 15%)

Molecular Weight Distributions of MWL and ILLs

The number-averaged molecular weight (M_n), weight-averaged molecular weight (M_w), and polydispersity index (PDI, M_w/M_n) of the MWL and ILLs were determined using GPC analysis, and the results are given in Table 3 and Fig. 3. The molecular weight distributions of the ILLs were compared with that of MWL. The M_w and PDI of MWL were 35,700 g/mol and 1.94, respectively. The M_w of the ILL treated with [EMIM]Ac decreased with increasing treatment temperature. The M_w of the ILLs treated at 60, 100, 120, and 140 ℃ were 131,700, 93,300, 55,100, and 29,500 g/mol, respectively. The M_w values of the ILLs treated with [EMIM]Ac, [AMIM]Cl, [BMIM]Cl, and [HMIM]Cl were 29,500, 28,000, 38,000, and 47,000, respectively. This indicates that the lignin structure degraded to the greatest extent under treatment with [AMIM]Cl. The highest PDI was obtained for the ILL treated with [EMIM]Ac at 60 ℃, representing the largest M_w range.

Table 3. Average Molecular Weights and PDI of MWL and ILLs

Sample	IL	Reaction Temperature (°C)	Mn (g/mol)	Mw (g/mol)	PDI
MWL	-	-	18,400	35,700	1.94
ILL	[EMIM]Ac	60	16,400	131,700	8.03
		100	15,700	93,300	5.94
		120	13,200	55,100	4.17
		140	11,500	29,500	2.57
	[AMIM]Cl	140	14,000	28,000	2.00
	[BMIM]Cl	140	15,200	38,000	2.50
	[HMIM]Cl	140	15,500	47,000	3.03

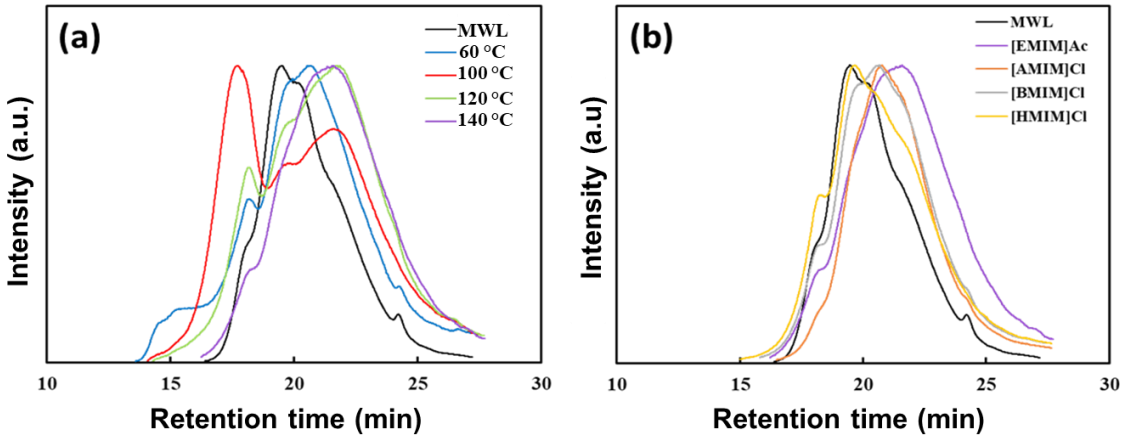

Fig. 3. Molecular weight distribution curves for MWL and ILLs obtained (a) at different treatment temperatures using [EMIM]Ac and (b) with four different types of ILs at 140 °C

Methoxyl Group Contents of MWL and ILLs

Table 4 presents the methoxyl group contents of the MWL and ILLs. The areas of CH_3I and IS were obtained through GC/FID analysis, and the weight of CH_3I was calculated based on the area ratio according to the calibration curve. The number of methoxyl groups in lignin could be obtained by dividing the weight of CH_3I by the molecular weight of CH_3I and multiplying by the dose used in the analysis.

Table 4. Methoxyl Group Contents of MWL and ILLs

Sample	IL	Temp. (°C)	Area		Area of CH_3I/IS	Weight CH_3I (mg)	Methoxyl Groups (mmol/g)
			CH_3I	IS			
MWL	-	-	42.38	7063.82	0.01	0.84	0.20
ILL	[EMIM]Ac	60	22.94	373.28	0.06	8.55	2.01
		100	22.92	222.31	0.10	14.34	3.37
		120	51.20	1288.47	0.04	5.53	1.30
		140	54.05	1333.52	0.04	5.64	1.32
	[AMIM]Cl	140	14.85	242.99	0.06	8.50	2.00
	[BMIM]Cl	140	14.66	234.13	0.06	8.71	2.05
	[HMIM]Cl	140	14.88	240.61	0.06	8.60	2.02

The methoxyl group content of MWL was 0.20 mmol/g. The methoxyl group contents of the ILLs treated with [EMIM]Ac at different temperatures (60, 100, 120, and 140 °C) were 2.01, 3.37, 1.30, 1.32 mmol/g, respectively. The highest methoxyl group content was obtained at 100 °C. The methoxyl group contents of the ILLs treated with [EMIM]Ac, [AMIM]Cl, [BMIM]Cl, and [HMIM]Cl under the same conditions were 1.32, 2.00, 2.05, and 2.02 mmol/g, respectively. The ILL treated with [BMIM]Cl had the highest methoxyl group content.

Hydroxyl Group Contents of MWL and ILLs

Figures 4 and 5 show ^{1}H NMR spectra of the MWL and ILLs. The signals at 4 to 3.5 ppm originated from methoxyl groups. The signals at 2.4 to 2.2 ppm and 2.2 to 1.8 ppm originated from phenolic hydroxyl and aliphatic hydroxyl groups, respectively. The ratios of the phenolic and aliphatic hydroxyl groups were calculated by setting the integral value of the methoxyl group region to 1. Then, the hydroxyl group contents were calculated based on the methoxyl group content obtained from the GC/FID analysis. Table 5 lists the methoxyl and hydroxyl group contents of the MWL and ILLs. The phenolic hydroxyl group contents of the ILLs treated with [EMIM]Ac at 60, 100, 120, and 140 °C were 0.92, 0.98, 0.22, and 0.16 mmol/g, respectively. The aliphatic hydroxyl group contents were 2.59, 3.27, 1.06, and 1.11 mmol/g, respectively. The phenolic hydroxyl group contents of the ILLs treated with [EMIM]Ac, [AMIM]Cl, [BMIM]Cl, and [HMIM]Cl were 0.16, 1.23, 1.25, and 1.17 mmol/g, respectively. The aliphatic hydroxyl group contents of the ILLs treated with [EMIM]Ac, [AMIM]Cl, [BMIM]Cl, and [HMIM]Cl were 1.11, 2.19, 2.62, and 2.79 mmol/g, respectively. The ILLs treated with [AMIM]Cl, [BMIM]Cl, and [HMIM]Cl had higher methoxyl and hydroxyl group contents than those treated with [EMIM]Ac.

Dissolution Mechanism of Lignin by ILs

In IL treatment, although the lignin dissolution mechanism is not well understood so far, it is proposed to be achieved by breaking the H-bonds in lignin and by combining the aromatic nucleus and aliphatic chain of lignin (Zhang *et al.* 2017). With a specific IL ([EMIM]Ac), ILL yield increased with increase in temperature. This can be ascribed to the increased reaction kinetics and decreased viscosity of IL. The significant increase at 140 °C can be associated with the glass transition temperature of lignin (Börcsök and Pásztory 2021). Imidazolium based ILs dissolve lignin through the aromatic π-π interactions with lignin aromatic rings. The variation in anion and cation structure can significantly influence the lignin dissolution capacity. In terms of cation, increased alkyl chain length is known to decrease the lignin dissolution capacity, whereas the presence of extra π-bonds can increase it by forming active π-π interactions with the phenolic groups of lignin (Usmani *et al* 2020). Hence the expected ILL yield would be in the order of [AMIM]Cl > [EMIM]Ac > [BMIM]Cl > [HMIM]Cl. However, from Table 2, it was found to be in the order of [EMIM]Ac >[AMIM]Cl > [BMIM]Cl > [HMIM]Cl. Highest lignin dissolution by [EMIM]Ac can be ascribed to the acetate anion. In contrast to chloride ion, the basicity of acetate anion is known to weaken the hydrogen bonding network between the components of biomass. The acetate ion can effectively attack hydrogen attached to β carbon of lignin leading to cleavage of β-O-4 bonds in lignin (Rashid *et al* 2021).

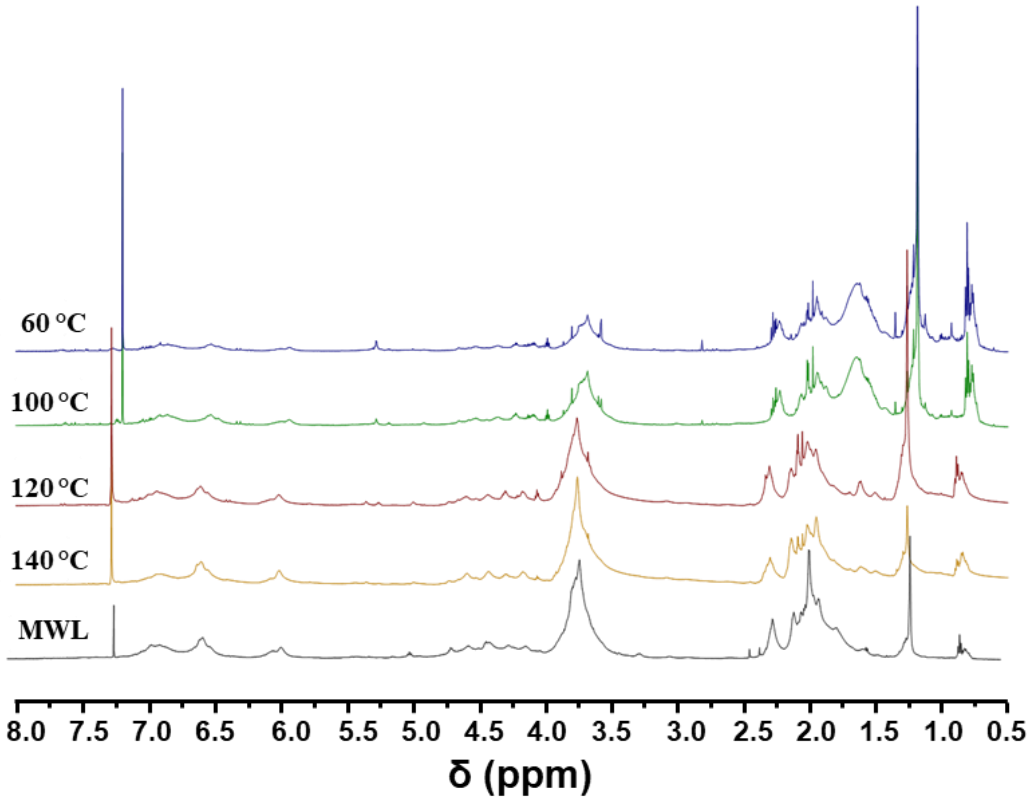

Fig. 4. ^{1}H NMR spectra of MWL and ILLs treated with [EMIM]Ac at different temperatures

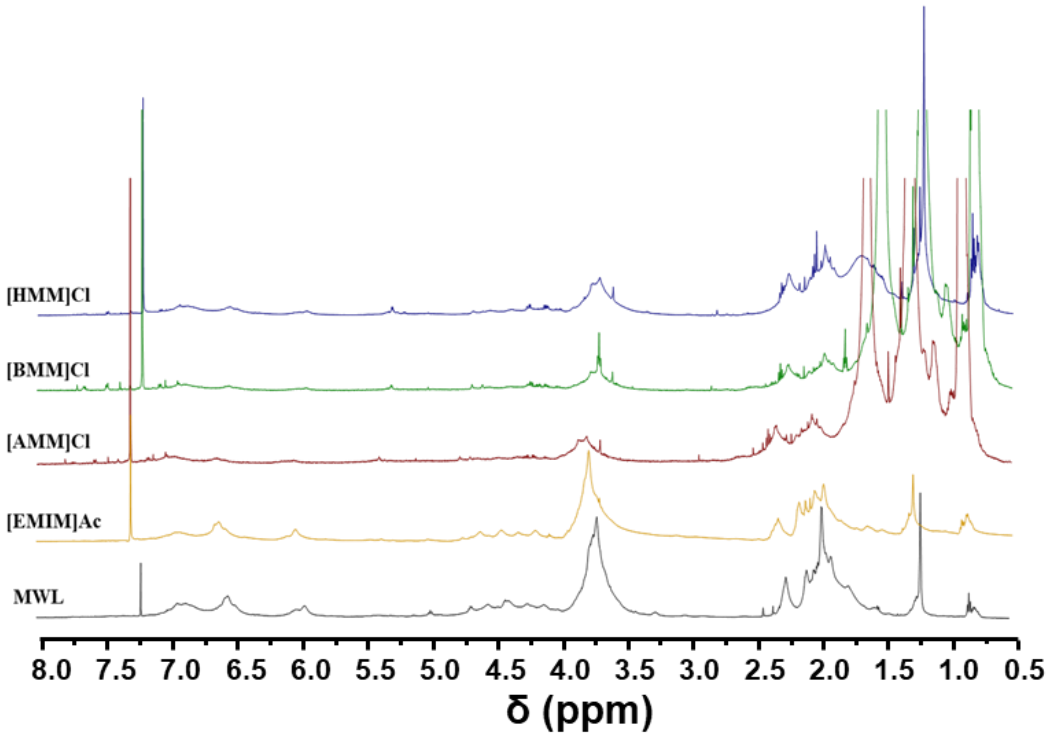

Fig. 5. ^{1}H NMR spectra of MWL and ILLs treated with different types of ILs at 140 °C

Table 5. Hydroxyl and Methoxyl Group Contents of MWL and ILLs

Sample	IL	Reaction Temperature (°C)	Methoxyl Groups (mmol/g)	Phenolic OH (mmol/g)	Aliphatic OH (mmol/g)	Total OH (mmol/g)
MWL	-	-	0.20	0.03	0.16	0.19
ILL	[EMIM]Ac	60	2.01	0.92	2.59	3.51
	-	100	3.37	0.98	3.27	4.24
	-	120	1.30	0.22	1.06	1.28
	-	140	1.32	0.16	1.11	1.27
	[AMIM]Cl	140	2.01	1.23	2.19	3.42
	[BMIM]Cl	140	2.05	1.25	2.62	3.87
	[HMIM]Cl	140	2.02	1.17	2.79	3.96

Structural Analysis of Esterified ILLs

Esterification with long chain fatty acids is known to improve the hydrophobicity and compatibility of lignin with other polymers. Hence, to further extend the applicability of ILL, esterification with three fatty acid chlorides of different molecular chain lengths (C8, C12, and C16) was performed. The ILLs esterified using octanoyl chloride (OC), lauroyl chloride (LC), and palmitoyl chloride (PC) are denoted as OC-ILL, LC-ILL, and PC-ILL, respectively. Figure 6 shows FT-IR spectra of ILL and esterified ILLs. The broad peaks in the range of 3200 to 3600 cm^{-1} are attributed to the stretching of the phenolic and aliphatic hydroxyl groups. The esterification reaction decreased this peak because the fatty acid ester was attached to the hydroxyl group. However, this decrease was much smaller than expected. As the carbon chain length of fatty acid chlorides increased, the intensity at 2937 cm^{-1}, which is attributed to C-H stretching, increased markedly compared to the unmodified ILL.

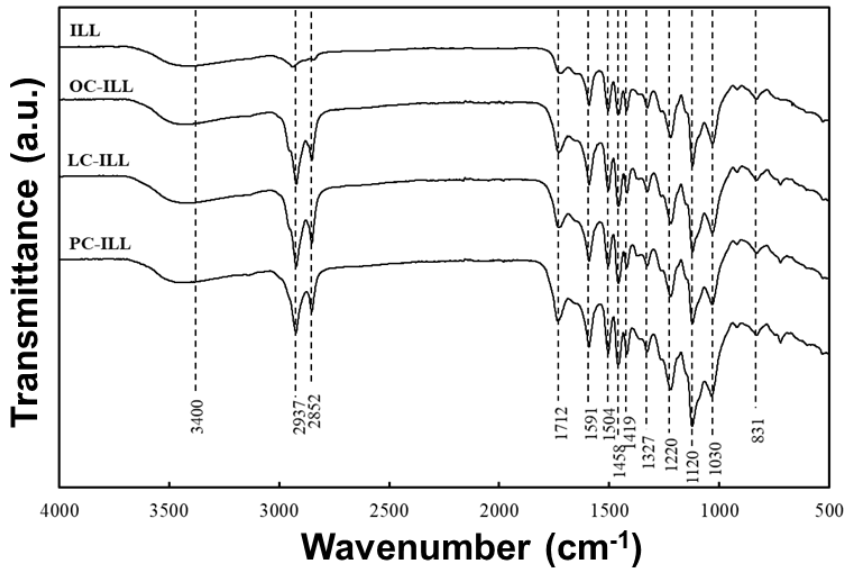

Fig. 6. FT-IR spectra of ILL and esterified ILLs

The peak at 1712 cm^{-1} is attributed to C=O stretching. The increase in this peak follows the decrease of the hydroxyl group. The peaks at 3400, 2937, 2852, and 1712 cm^{-1} are the most prominent peaks in the esterified ILLs compared to the unmodified ILL. The peaks at 1591, 1504, and 1419 cm^{-1} are attributed to aromatic skeletal vibration and are typical peaks of lignin. The peak at 1458 cm^{-1} corresponds to C-H deformation. The peaks at 1220 and 1120 cm^{-1} are assigned to C-O stretching vibrations.

Figure 7 shows ^{1}H NMR spectra of the acetylated ILL and esterified ILLs. The signal at 4 to 3.5 ppm originates from methoxyl groups. The signals at 2.4 to 2.2 ppm and 2.2 to 1.8 ppm originate from phenolic hydroxyl groups and aliphatic hydroxyl groups, respectively.

The peak at 1.3 ppm is assigned to methylene protons on a secondary carbon. As a result of esterification, the peaks at alkyl groups of esterified ILLs appear more prominent than in the unmodified ILL.

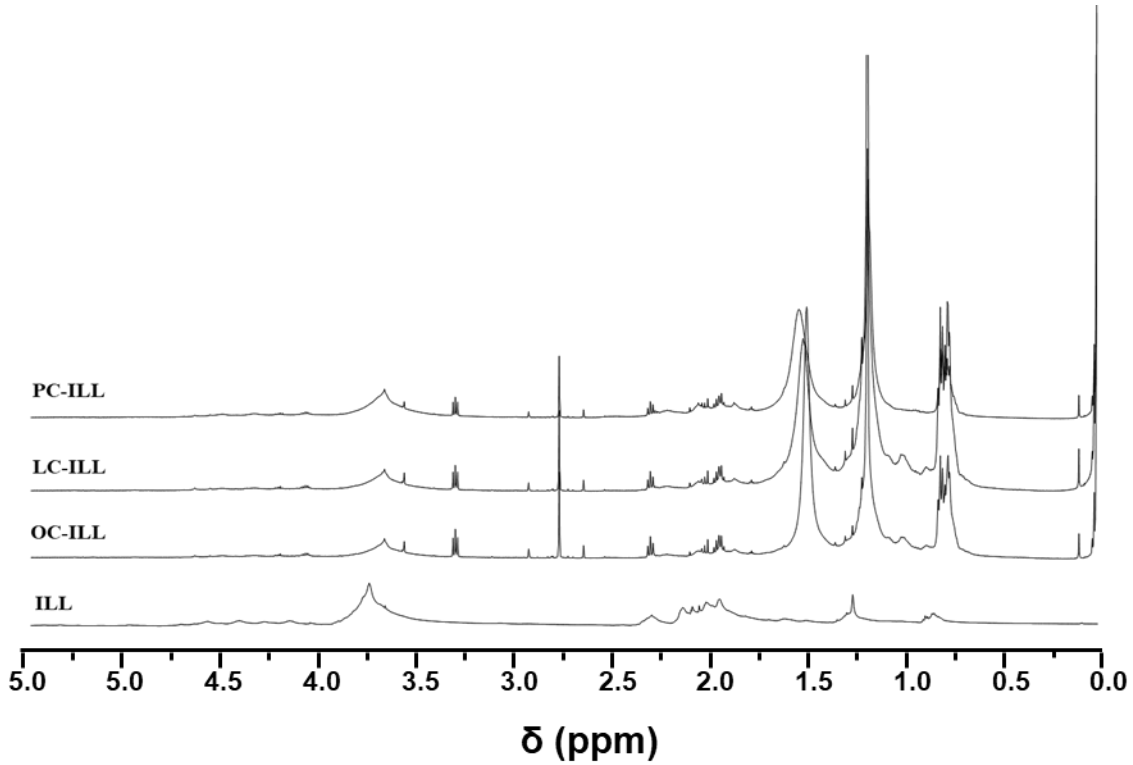

Fig. 7. ^{1}H NMR spectra of the acetylated ILL and esterified ILLs

Molecular Weight Distributions of Esterified ILLs

Figure 8 and Table 6 present the molecular weight and PDI of the acetylated ILL and esterified ILLs. The M_w of the esterified ILL is larger than that of the acetylated ILL, which is due to the successful esterification. The M_w of the esterified ILLs increases with increasing molecular chain length of the fatty acid chlorides. The M_w values of OC-ILL, LC-ILL, and PC-ILL were 33,200, 38,000, and 51,700 g/mol, respectively.

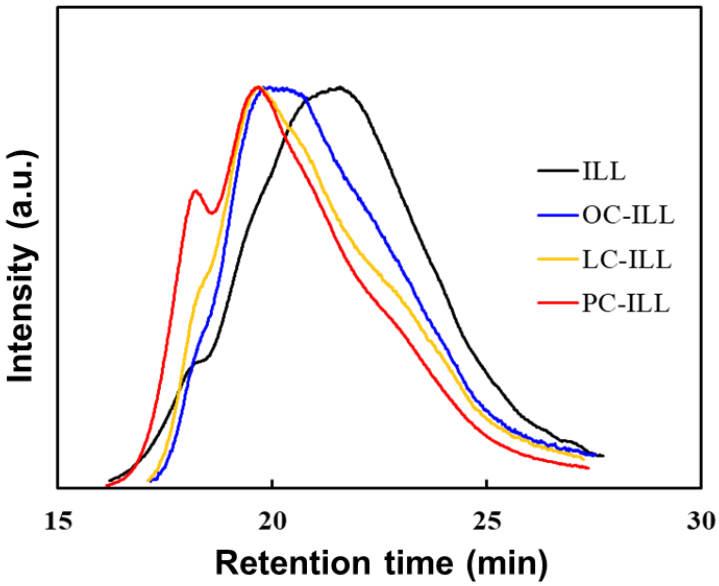

Fig. 8. Molecular weight distribution curves for the acetylated ILL and esterified ILLs

Table 6. Molecular Weight and PDI of the Acetylated ILL and Esterified ILLs

Sample	M_n (g/mol)	M_w (g/mol)	PDI
Acetylated ILL	11,500	29,500	2.57
OC-ILL	14,800	33,200	2.24
LC-ILL	16,200	38,000	2.35
PC-ILL	19,400	51,700	2.66

Thermal Degradation Behavior

Figure 9 shows thermogravimetry (TG) and derivative thermogravimetry (DTG) curves for ILL and the esterified ILLs. The ILL showed a slight weight loss below 100 °C corresponding to the evaporation of moisture. The esterified ILLs exhibited a smaller weight loss in this region because of their hydrophobicity. The greatest weight loss appeared between 200 and 400 °C in all samples. The thermal degradation of the esterified ILLs was greater than that of ILL, which may be associated with the loss of the introduced long aliphatic chain by the cleavage of the C-O bond in the ester linkage (Gordobil *et al.* 2016). Table 7 lists the thermal degradation temperatures at weight losses of 10%, 30%, and 50%, which are denoted as $T_{10\%}$, $T_{30\%}$, and $T_{50\%}$, respectively. The initial degradation temperatures at 10 wt% in the esterified ILLs were higher than that for the ILL. After 30% weight loss, the degradation temperatures of the esterified ILLs were lower than that for the ILL. All these analysis confirm the successful esterification of ILL and the results are in well accordance with the previous reports (Koivu *et al*. 2016). Hence the esterified ILLs have the potential to apply in preparing composites with other polymers.

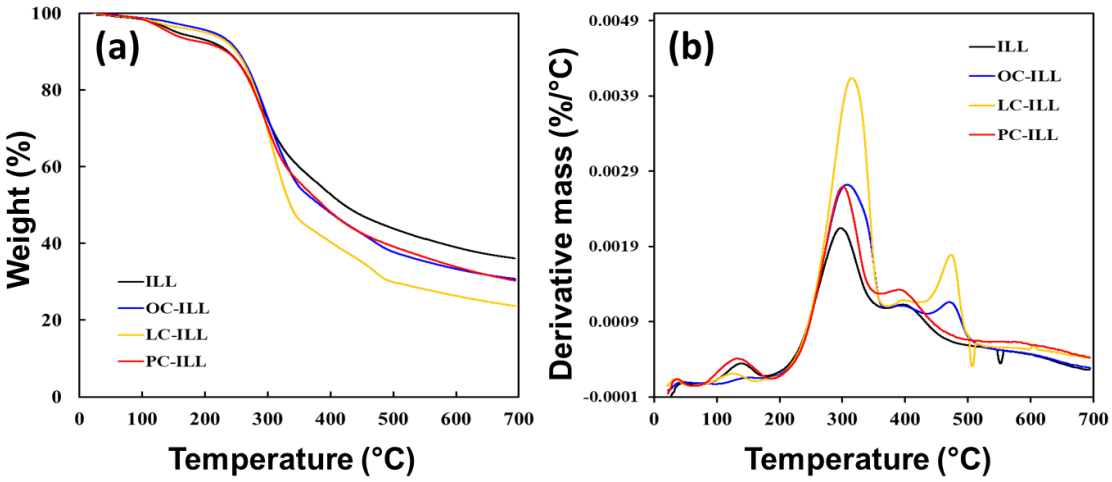

Fig. 9. (a) Thermogravimetry (TG) and (b) derivative TG (DTG) curves for ILL and esterified ILLs

Table 7. Thermogravimetric Results for ILL and Esterified ILLs

Sample	Degradation Temperature at Weight Loss Percentage (°C)		
	$T_{10\%}$	$T_{30\%}$	$T_{50\%}$
ILL	237	307	422
OC-ILL	253	306	384
LC-ILL	250	299	336
PC-ILL	234	301	388

CONCLUSIONS

1. Lignin was successfully isolated from lignocellulose using four types of ionic liquids (ILs), and the resulting material was thoroughly characterized using various techniques and compared with milled wood lignin (MWL).
2. All the ILLs showed Fourier transform infrared (FT-IR) peaks similar to those of MWL, indicating a similar structure to MWL.
3. The M_w of ILLs treated with [EMIM]Ac and [AMIM]Cl were 29,500 and 28,000 g/mol, respectively, and showed low polydispersity index (PDI) values.
4. The functional group contents of the ILLs decreased as the treatment temperature increased. A methoxyl group content of 1.32 mmol/g and total hydroxyl group content of 1.27 mmol/g were obtained in the ILL treated with [EMIM]Ac at 140 °C.
5. The ILL was successfully esterified using three fatty acid chlorides. The M_w increased as the molecular chain length of the fatty acid chlorides increased. The M_w values of ILL, OC-ILL, LC-ILL, and PC-ILL were 29,500, 33,200, 38,000, and 51,700 g/mol, respectively.

ACKNOWLEDGMENTS

This research was supported by the Basic Science Research Program through the National Research Foundation of Korea (NRF), funded by the Ministry of Education (No. 2018R1A6A1A03025582) and by the National Institute of Forest Science (Grant No. FP0701-2021-02).

REFERENCES CITED

An, Y. X., Zong, M. H., Wu, H., and Li, N. (2015). "Pretreatment of lignocellulosic biomass with renewable cholinium ionic liquids: Biomass fractionation, enzymatic digestion and ionic liquid reuse," *Bioresource Technology* 192, 165-171. DOI: 10.1016/j.biortech.2015.05.064

Audu, I. G., Ziegler-Devin, I., Winter, H., Bremer, M., Hoffmann, A., Fischer, S., Laborie, M.-P., and Brosse, N. (2017). "Impact of ionic liquid 1-ethyl-3-methylimidazolium acetate mediated extraction on lignin features," *Green and Sustainable Chemistry* 7(2), 114-140. DOI: 10.4236/gsc.2017.72010

Awal, A., and Sain, M. (2011). "Spectroscopic studies and evaluation of thermorheological properties of softwood and hardwood lignin," *Journal of Applied Polymer Science* 122(2), 956-963. DOI: 10.1002/app.34211

Brandt, A., Gräsvik, J., Hallett, J. P., and Welton, T. (2013). "Deconstruction of lignocellulosic biomass with ionic liquids," *Green Chemistry* 15(3), 550-583. DOI: 10.1039/c2gc36364j

Börcsök, Z., and Pásztory, Z. (2021). "The role of lignin in wood working processes using elevated temperatures: An abbreviated literature survey," *European Journal of Wood and Wood Products* 79(3), 511-526. DOI: 10.1007/s00107-020-01637-3

Cateto, C. A., Barreiro, M. F., Rodrigues, A. E., and Belgacem, M. N. (2011). "Kinetic study of the formation of lignin-based polyurethanes in bulk," *Reactive and Functional Polymers* 71(8), 863-869. DOI: 10.1016/j.reactfunctpolym.2011.05.007

Delmas, G. H., Benjelloun-Mlayah, B., Bigot, Y. L., and Delmas, M. (2013). "Biolignin TM based epoxy resins," *Journal of Applied Polymer Science* 127(3), 1863-1872. DOI: 10.1002/app.37921

Dong, S. J., Zhang, B. X., Gao, Y. F., and Hu, X. M. (2015). "An efficient process for pretreatment of lignocelluloses in functional ionic liquids," *International Journal of Polymer Science* 2015, article ID 978983. DOI: 10.1155/2015/978983

Gordobil, O., Robles, E., Egüés, I., and Labidi, J. (2016). "Lignin-ester derivatives as novel thermoplastic materials," *RSC Advances* 6(90), 86909-86917. DOI: 10.1039/c6ra20238a

Isikgor, F. H., and Becer, C. R. (2015). "Lignocellulosic biomass: A sustainable platform for the production of bio-based chemicals and polymers," *Polymer Chemistry* 6(25), 4497-4559. DOI: 10.1039/c5py00263j

Koivu, K. A. Y., Sadeghifar, H., Nousiainen, P. A., Argyropoulos, D. S., and Sipilä, J. (2016). "Effect of fatty acid esterification on the thermal properties of softwood kraft lignin," *ACS Sustainable Chemistry and Engineering* 4(10), 5238-5247. DOI: 10.1021/acssuschemeng.6b01048

Rashid, T., Sher, F., Rasheed, T., Zafar, F., Zhang, S., and Murugesan, T. (2021). "Evaluation of current and future solvents for selective lignin dissolution – A

review," *Journal of Molecular Liquids* 321, article no. 114577. DOI: 10.1016/j.molliq.2020.114577.

Sannigrahi, P., Pu, Y., and Ragauskas, A. (2010). "Cellulosic biorefineries-unleashing lignin opportunities," *Current Opinion in Environmental Sustainability* 2(5-6), 383-393. DOI: 10.1016/j.cosust.2010.09.004

Sathitsuksanoh, N., Holtman, K. M., Yelle, D. J., Morgan, T., Stavila, V., Pelton, J., Blanch, H., Simmons, B. A., and George, A. (2014). "Lignin fate and characterization during ionic liquid biomass pretreatment for renewable chemicals and fuels production," *Green Chemistry* 16(3), 1236-1247. DOI: 10.1039/c3gc42295j

Su, Y., Yang, B., Liu, J., Sun, B., Cao, C., Zou, X., Lutes, R., and He, Z. (2018). "Prospects for replacement of some plastics in packaging with lignocellulose materials: A brief review," *BioResources* 13(2), 4550-4576. DOI: 10.15376/BIORES.13.2.SU

Tanase-Opedal, M., Espinosa, E., Rodríguez, A., and Chinga-Carrasco, G. (2019). "Lignin: A biopolymer from forestry biomass for biocomposites and 3D printing," *Materials* 12(18), article no. 3006. DOI: 10.3390/ma12183006

Tarasov, D., Leitch, M., and Fatehi, P. (2018). "Lignin-carbohydrate complexes: Properties, applications, analyses, and methods of extraction: A review," *Biotechnology for Biofuels* 11(1), article no. 269. DOI: 10.1186/s13068-018-1262-1

Usmani, Z., Sharma, M., Gupta, P., Karpichev, Y., Gathergood, N., Bhat, R., and Gupta, V. K. (2020). "Ionic liquid based pretreatment of lignocellulosic biomass for enhanced bioconversion," *Bioresource Technology* 304, article no. 123003. DOI: 10.1016/j.biortech.2020.123003

Vanholme, R., Demedts, B., Morreel, K., Ralph, J., and Boerjan, W. (2010). "Lignin biosynthesis and structure," *Plant Physiology* 153(3), 895-905. DOI: 10.1104/pp.110.155119

Xu, J. K., Sun, Y. C., and Sun, R. C. (2015). "Synergistic effects of ionic liquid plus alkaline pretreatments on eucalyptus: Lignin structure and cellulose hydrolysis," *Process Biochemistry* 50(6), 955-965. DOI: 10.1016/j.procbio.2015.03.014

Yang, J., Ching, Y. C., and Chuah, C. H. (2019). "Applications of lignocellulosic fibers and lignin in bioplastics: A review," *Polymers* 11(5), article no. 751. DOI: 10.3390/polym11050751

You, T. T., Zhang, L. M., Zhou, S. K., and Xu, F. (2015). "Structural elucidation of lignin-carbohydrate complex (LCC) preparations and lignin from *Arundo donax* Linn," *Industrial Crops and Products* 71, 65-74. DOI: 10.1016/j.indcrop.2015.03.070

Yu, O., and Kim, K. H. (2020). "Lignin to materials: A focused review on recent novel lignin applications," *Applied Sciences (Switzerland)* 10(13), article no. 4626. DOI: 10.3390/app10134626

Yuan, W. L., Yang, X., He, L., Xue, Y., Qin, S., and Tao, G. H. (2018). "Viscosity, conductivity, and electrochemical property of dicyanamide ionic liquids," *Frontiers in Chemistry* 6, article no. 59. DOI: 10.3389/fchem.2018.00059

Zakzeski, J., Bruijnincx, P. C. A., Jongerius, A. L., and Weckhuysen, B. M. (2010). "The catalytic valorization of lignin for the production of renewable chemicals," *Chemical Reviews* 110(6), 3552-3599. DOI: 10.1021/cr900354u

Zhang, P., Dong, S. J., Ma, H. H., Zhang, B. X., Wang, Y. F., and Hu, X. M. (2015). "Fractionation of corn stover into cellulose, hemicellulose and lignin using a series of ionic liquids," *Industrial Crops and Products* 76, 688-696. DOI: 10.1016/j.indcrop.2015.07.037

Zhang, Q., Hu, J., and Lee, D. J. (2017). "Pretreatment of biomass using ionic liquids: research updates," *Renewable Energy* 111, 77-84. DOI: 10.1016/j.renene.2017.03.093

Article submitted: May 3, 2022; Peer review completed: July 30, 2022; Revised version received and accepted: August 8, 2022; Published: August 25, 2022.
DOI: 10.15376/biores.17.4.5861-5877